CHAPTER- 2

Literature review

2.1. Introduction

NO_x emission from stationary and automobiles sources cause environmental pollution, including acid rain, photochemical smog, ozone layer depletion, and global warming. Selective catalytic reduction (SCR) with NH_3 as a reducing agent is a well-known technology to convert NO_x into N_2 and H_2O. [1,2]

The activity improvement and increased N_2 selectivity at low and medium temperatures are key characteristics in developing NH_3-SCR catalysts for stationary and automotive applications. The various NO_x reduction catalytic systems implemented for the NH_3-SCR process are described in detail in this chapter.

2.2. Reaction Mechanism of NH_3-SCR

NH_3-SCR technology is currently the most significant technology to control NO_x emissions. In the SCR system, the main reactants are NO, NO_2 and O_2 in the flue gas and the reductant is NH_3. The NH_3-SCR reaction may varies depending on the content of NO and NO_2 in the exhaust gas and main reactions involved in the NH_3-SCR process are as follows:

$$4NO + 4NH_3 + O_2 \rightarrow 4N_2 + 6H_2O \quad (2.1)$$

$$2NO_2 + 4NH_3 + O_2 \rightarrow 3N_2 + 6H_2O \quad (2.2)$$

$$4NH_3 + 2NO + 2NO_2 \rightarrow 4N_2 + 6H_2O \quad (2.3)$$

$$6NO + 4NH_3 \rightarrow 5N_2 + 6H_2O \quad (2.4)$$

$$6NO_2 + 8NH_3 \rightarrow 7N_2 + 12H_2O \quad (2.5)$$

Equations (2.1) -(2.5) occur in the presence and absence of O_2 that results in reduction of NOx. Due to the equal NO: NH_3 ratio in its stoichiometry, reaction (2.1) is known as "Standard SCR" reaction category. Above 200°C, the reaction (2.3) is known as a "Fast SCR" reaction since it has ten times the efficiency of the reaction (2.1). [3,4]

2.3. Catalysts used in NH_3-SCR

The SCR catalyst is the heart of the SCR system, consisting of active metal and support. The catalysts in the NH_3-SCR system improve the active temperature window, N_2 selectivity, sulphur and water tolerance and life cycle of the catalysts. Depending upon the composition, the NH_3-SCR catalyst can be divided into the following categories, shown in the **Fig.2.1**.

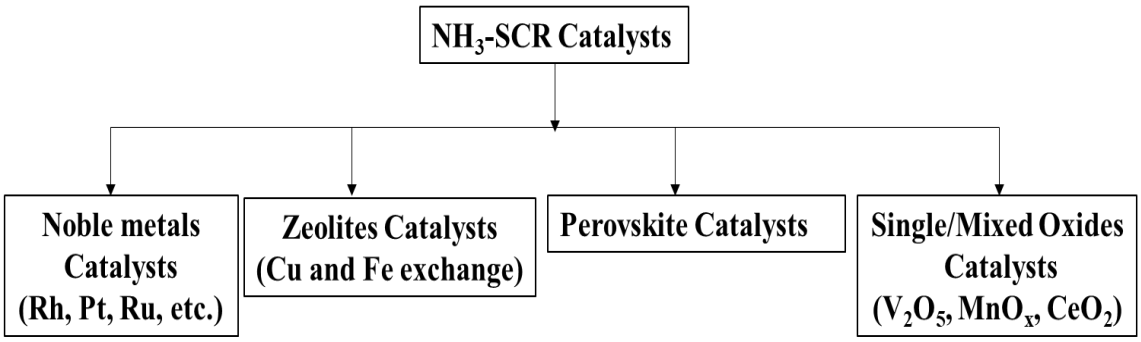

Fig. 2.1. Different groups of catalysts used in NH_3-SCR process

2.3.1. Nobel metals-based catalysts

Noble metals were the first commonly used catalysts in the SCR system because of their outstanding activity at low temperatures. Noble metal catalysts exhibited consistent catalytic activity throughout various environmental conditions, along with exceptional resistance to oxidation, corrosion, and high temperatures. NH_3-SCR studies on noble metals-based catalysts are summarized in **Table 2.1**.

Table 2.1. An overview of NH_3-SCR noble metal catalysts

Catalysts	Feed gas condition Temperature Window	Remarks	Ref.
Pt/Al_2O_3 (Ion exchange method)	NH_3 = 500 ppm NO= 500 ppm O_2 = 5vol.% GHSV = 100,000 h^{-1} (100-500 °C)	Pt/Al_2O_3 gave the highest NO_x conversion at 200°C. Beyond 200°C, NO_x conversion started decline	[5]
Ag/MgO-Al_2O_3 (Impregnation method)	NO=83 ppmv NH_3= 237 ppmv O_2=10% v/v O_2 GHSV = 96,000h^{-1} (100-500°C)	MgO in the catalysts affected the NO conversion. High NH_3-SCR and NO oxidation activity for low Ag loadings and catalysts showed high thermal stability.	[6]
Ag–Mn–Ce/γ-Al_2O_3 (Sol-gel methods)	NH_3 = 700 ppm NO= 700 ppm O_2= 3vol.% Total flow rate = 1000ml-min^{-1} (100 -450 °C)	In the Ag–Mn–Ce/γ-Al_2O_3 catalyst when Ag was 2wt.% Ag, 95% NO conversion was obtained in 250–300°C temperature range, and demonstrated good GHSV tolerance over a broad temperature range.	[7]
RuNi/Al-SBA-15 (Impregnation method)	NO = 627 ppm NH_3 = 600ppm O_2= 1.7 – 7 vol.% GHSV =32,500–54,000 ml h^{-1} (100-400 °C)	RuNi/Al-SBA-15 catalyst showed 90.2% NO conversion at 300°C in excess oxygen conditions (7%) and ruthenium enhanced activity which were correlated with the catalyst's physicochemical properties and excellent textural properties.	[8]
CeO_x–MnO_x–RuO_x/TiO_2 (Impregnation method)	NO = 550 ppm, NH_3 = 550ppm, O_2 = 10vol.%, GHSV =23,000 h^{-1} (50-350°C)	The CeO_x–MnO_x–RuO_x/TiO_2 catalyst calcined at 350 °C exhibited the highest denitrification efficiency (100%) at 120°C.	[9]

Baik et al. [5] synthesized Pt/Al_2O_3 catalysts through wet-impregnation for NO removal in a packed-bed flow reactor system. The Pt/Al_2O_3 catalyst exhibited NO conversion more than 60% at 150℃ and after 200℃ temperatures, the NO_x conversion started to decline. Cao et al. [7] synthesized Ag–Mn–Ce/γ-Al_2O_3 catalyst for NH_3-SCR and showed excellent activity at low and middle temperatures, and exhibited 95% NO conversion at 250°C. The silver is mainly present in Ag and Ag_2O, which may promote the migration of surface-active oxygen and lead to an increase in weak Brønsted and strong Lewis's acid sites. Perumal et al. [8] used Ru-Ni/Al-SBA-15 catalyst to reduce nitric oxide by SCR. Using excess oxygen (7%) and with addition of ruthenium as promoter, the catalyst showed superior performance at 300°C; achieving more than 90% conversion. Ren et al. [9] synthesized CeO_x–MnO_x–RuO_x/TiO_2 catalyst by the impregnation method. The catalyst was calcined at different temperatures and the catalyst calcined at 350°C exhibited the highest rate of low-temperature (120°C) denitration activity. The characterization results showed that Ce^{4+}, Mn^{4+}, Ru^{4+}, and lattice oxygen, significantly improved the catalyst's ability to activate NO, promoting the NH_3-SCR reaction. The catalyst calcined at 250°C possessed the competitive adsorption sites for NO and NH_3 molecules, whereas catalyst calcined at 350 and 450°C temperatures showed active sites for adsorption.

The literature studies on noble metal catalysts have shown high catalytic activity at low temperatures. However, due to their high cost and limited active window, they are inappropriate for treating NO_x for large-scale stationary sources. As a result, metal oxide catalysts progressively replaced noble metal catalysts, which are now limited to low-temperature catalysis and the treatment of vehicle exhaust gases.

2.3.2. Single oxides/mixed oxides-based catalysts

2.3.2.1. Vanadium based catalysts

In recent decades, vanadium-based catalysts have been used as industrial SCR catalysts to exhibit higher than 90% NO_x removal efficiency at operating temperatures of 350–400℃. However, activity of vanadium catalyst is poor at high temperature. Hence many researchers focussed on modified V- based catalyst to meet stringent emission requirement. Various composition of vanadium-based catalysts used such as composite vanadium-based oxide catalysts, supported vanadium-based catalysts have been synthesized for NO removal by NH_3-SCR technique [10,11], which is summarized in the **Table 2.2**.

A significant amount of research has been done on composite vanadium-based oxide catalysts in recent decade for NO_x removal with NH_3. Zhang et al. [17] reported that a Fe-V-O mixed oxide synthesized via co-precipitation has a broad operating temperature window. More than 80% NO conversion was attained between 210-400°C. Chen et al. [18] synthesized Ti-V-O catalyst. The results showed that between 200-400°C, Ti-V-O catalysts could convert more than 80% of the NO.

Additionally, over the past few decades various supports have been extensively developed such as Al_2O_3 [19–21], TiO_2 [22,23], Activated charcoal [24,25], CNTs [26,27] and other metal oxides [28,29] to improve and optimize V-based catalysts. The role of γ-Al_2O_3 support has been reported by Huang et al. [6]. The results suggested that γ-Al_2O_3 provided large specific area, improves the dispersion of V_2O_5 species, and facilitated the formation of reduced vanadium species and enhanced catalytic activity of vanadium-based catalysts for NH_3-SCR. TiO_2 is an exciting support of SCR catalysts because they have many properties, such as being less acidic, providing a uniform dispersion of active metals, and only weakly and reversibly sulphated [30].

Table 2.2. The catalysts based on vanadium in NH_3-SCR

Catalysts Preparation Techniques	Feed gas conditions Temperature window	Remarks	Ref.
V_2O_5 (Impregnation method)	NO=500 ppm NH_3=500 ppm O_2=5 vol.% GHSV=50,000h^{-1} (150-450°C)	100% NO_x conversion was achieved in the temperature range of 150-450°C. The high redox properties improved the catalytic performance of the catalyst.	[12]
Fe–V–O_x (Co-precipitation method)	NO= 500 ppm NH_3=500 ppm O_2= 5 vol.% (100 to 400°C)	In the temperature range of 150-250 °C catalyst showed more than 90% NO_x conversion. The high acidity and redox ability were the factors, which enhanced the performance of Fe–V–O_x catalyst	[13]
MoO_3-V_2O_5/Al_2O_3 (Impregnation method)	NO=500 ppm NH_3= 500 ppm O_2 =10vol.% GHSV=25,000h^{-1} (200 to 450°C)	The addition of MoO_3 enhanced the catalytic activity, whereas the particle size of V_2O_5 was decreased, which enhanced the BET surface area. It also exhibited excellent resistance to SO_2	[14]
V_2O_5/WO_3-TiO_2 (Hydrothermal method)	NO=500 ppm NH_3=500 ppm O_2=5vol.% GHSV=50000 h^{-1} (250–550°C)	The catalyst displayed high NO conversion at 250–550°C. Compared to the high-valence vanadium species (V^{5+}), the low-valence vanadium species (V^{3+}) showed significantly greater SCR activity.	[15]
V_2O_5-MoO_3/TiO_2 (Wet-impregnation method)	NO=0.05% NH_3=0.05% O_2=4 vol.% GHSV=30000 h^{-1}	Mg-V_2O_5-MoO_3/TiO_2 catalysts showed a higher P, SO_2, and H_2O resistance than V_2O_5-MoO_3/TiO_2.The highest NO_x conversion of 97.5% was achieved at 350°C.	[16]

Takagi et al. [31] examined the catalytic activity of vanadium-based catalysts for NH_3-SCR on various supports (Al_2O_3, SiO_2, and TiO_2). The experimental results revealed that for the

supported catalysts, the ammonia adsorption (NH^{4+}) reactivity for NO_2 was in the following ascending order: TiO_2 > Al_2O_3 > SiO_2. Also, TiO_2 catalysts were more effective than Al_2O_3 catalysts in dispersing V_2O_5 and thereby enhancing redox ability and total acidity of the catalysts. A nanostructure of V_2O_5/TNTs-Al_2O_3 catalyst with excellent catalytic activity was synthesized by Camposeco et al. [32]. The catalyst was used over a wide temperature range of 280 to 480°C and accomplishes more than 80% of the NO conversion.

2.3.2.2. Manganese based catalysts

Several studies have found that Mn-based catalysts perform better at low temperatures than standard catalysts for SCR reaction. In the literature, Mn-based catalysts have shown excellent activity due to its outstanding redox ability and variable valence states, which are important for low-temperature SCR. The crystallinity, specific surface area, oxidation state, active oxygen, active sites, and acidity on the surface influenced the catalytic activity. In actual conditions, H_2O and SO_2 poisoning or inhibition severely affect pure MnO_x catalysts. Research on supported catalysts and other metal oxides based on manganese has been conducted to improve the stability and resistance of the catalysts. [33,34] The catalysts based on manganese in NH_3-SCR are summarized in the **Table 2.3**.

Table 2.3. Review on manganese-based catalysts in NH_3-SCR studies

Catalysts Preparation Techniques	Reactant conditions Temperature window	Remarks	Ref.
Amorphous MnO_x (Rheological phase reaction method, Low temperature solid phase reaction method, Co-precipitation method	NO=500 ppm NH_3= 500 ppm O_2= 3% GHSV=47,000 h^{-1} (50-150°C)	The results shows that the catalysts exhibit excellent low temperature activity; at 80°C, the NO_x conversion is approximately 98%, and between 100-150°C, it is close to 100%.	[33]
Novel MnO_x (Precipitation method)	NO=500 ppm NH_3=500 ppm O_2=5 vol.% GHSV=25,000 h^{-1} (348-523°K)	Outstanding catalytic activity in the 348–473°K temperature range. With the 20% water vapor the catalysts also showed excellent performance.	[34]
Different crystal structure of MnO_2 (Hydrothermal method)	NO = 720 ppm NH_3 = 800 ppm O_2 = 3 vol.% GHSV =30 000 h^{-1} (80-200°C)	NO_x conversion efficiency was in the order of γ-MnO_2 > α-MnO_2 > δ-MnO_2 > β-MnO_2. In the 140–200°C temperature range, 90% was achieved by the γ-MnO_2 and α-MnO_2 catalysts.	[35]
Nano-Fe-Mn oxides (Thermal treatment method)	NO=1000 ppm NH_3= 1000 ppm O_2=3 vol.% GHSV=72,000 h^{-1} (100–300°C)	Fe-Mn oxides catalyst synthesized through the thermal treatment at 300°C exhibited an excellent NO (90%) conversion in the temperature range of 130-300°C.	[36]
Mn-FeV (One pot methods)	NO=500 ppm NH_3=500 ppm O_2=3 vol.% GHSV=40,000 h^{-1} (100-400°C)	The 0.3Mn-FeV catalyst achieved 100% NO_x conversion at 250°C, and excellent N_2 selectivity in the NH_3-SCR process. It also shows the good SO_2 tolerance.	[37]

Mn-Ce-Co (co-precipitation method)	NO=500 ppm NH_3=500 ppm O_2=5vol.%, GHSV= (40-100) $x10^3$ h^{-1} (50-350℃)	The results shows that the HPW-Mn-Ce-Co catalyst has the highest surface acidity, and oxygen vacancies, due to which higher NO_x conversion (~100% at 100–250°C) and N_2 selectivity (more than 80% at 50–350°C).	[38]
Mn-RE/TiO_2 (RE = Ce, Sm, Nd, Er, Y) (Impregnation method, Coprecipitation method, Sol-gel method)	NO= 600 ppm NH_3= 600 ppm O_2 = 3 vol.% GHSV=40,000 h^{-1} (40 to 400°C)	The 30% Mn-3% Nd/TiO_2 catalyst shows the 100% of NO_x conversion in the 100-320°C temperature range. They also found the good SO_2 tolerance.	[39]
MnO_x/CeO_2–ZrO_2–Al_2O_3 (Wet impregnation method)	NO=1000 ppm NH_3=1000 ppm O_2=5vol.% GHSV=10,000 h^{-1} (500-350℃)	The most active catalyst is MnO_x/CZA with 10% manganese loading; in the temperature range of 143–300°C, over 90% of NO is converted to N_2.	[40]

2.3.2.2.1. Single manganese oxide catalysts

MnO_x has a significant redox ability and surface acidity due to the interconversion of Mn^{n+} ions with different valences, which improves the low-temperature SCR performance of MnO_x-based catalysts. The efficiency and N_2 selectivity of single-component MnO_x catalysts in the SCR process is proportional to the oxidation state of the catalyst. Compared to Mn_2O_3 and Mn_3O_4, MnO_2 exhibited higher SCR performance across a broad temperature range. At 125°C to 250°C, the NO conversion exceeded 90%, primarily because of the greater oxidation and superior catalytic activity of the high-valence Mn^{4+} ions. As a result, MnO_2 has shown best SCR activity among the single-component MnO_x. Kapteijn et al.'s [41] investigated SCR

activity of MnO_x in various valence states and observed the activity in the following order: $MnO_2 > Mn_5O_8 > Mn_2O_3 > Mn_3O_4$.

MnO_2's crystalline phase was an important factor influencing the de-NO_x activity. According to Gong et al. [42], the NO_x conversion rates of MnO_2 catalysts with various structures were as follows: γ-MnO_2 > α-MnO_2 > δ-MnO_2 > β-MnO_2. The γ-MnO_2 catalyst showed the highest NO_x conversion, and the N_2 selectivity of the γ- and α-MnO_2 catalysts was over 90% in the 140–200°C temperature range. Shao et al. [43] synthesized the α-MnO_2, β-MnO_2, γ-MnO_2, and δ-MnO_2 catalysts to study the interaction effect on the simultaneous catalytic oxidation of NO. At 250°C, the γ-MnO_2 reached its maximum conversion of 92.1%, and from 220°C to 340°C. The specific surface area, surface acidity, and morphology of single manganese oxide catalysts also have a significant impact on their physicochemical properties and catalytic activity. The catalyst with a higher specific surface area could expose more active sites on the surface which can enhance the catalyst's SCR performance. [44,45] The NH_3 adsorption is enhanced by the significant surface acidity, which in turn improves SCR efficiency. Manganese oxide materials with spherical, rod-like, and nano-flower morphologies showed superior catalytic performance compared to bulk particles. [46] This was explained by the fact that the latter had a lower Mn–O binding strength and more surface defect sites, which increased the number of active canters and made it easier to produce more surface-adsorbed oxygen (O_α). While the single MnO_x catalyst exhibits satisfactory catalytic performance at low temperatures, there are still several ways to further increase the NH_3-SCR's low-temperature activity, such as addition of other transition metal or MnO_x deposition onto support.

2.3.2.2.2. Composite manganese oxide-based catalysts

When Ce, Co, Sm, Sb, Eu, Ni, and other metal components were doped on pure MnO_x, the SCR activity significantly improved. The adsorption of the reactants (NH_3 and NO) at the active site was facilitated by the doping of metals, which also enhanced the specific surface

area of the catalyst and improved the dispersity of the activated components. CeO_2 has superior oxygen storage and evolution capacity and is used as a modifier for MnO_x-based catalysts. A small amount of the Ce^{4+} within the crystal becomes Ce^{3+}, generating oxygen vacancies, and releases lattice oxygen and transforms it into surface-adsorbed oxygen.[47] When the atmosphere is abundant in oxygen, CeO_2 will simultaneously transform the adsorbed oxygen back into lattice oxygen for storage and Ce^{3+} back into Ce^{4+}. It also decreased the low-temperature SCR reaction's apparent activation energy.[48] The Co-Mn bimetallic catalyst demonstrated higher stability and reducibility when compared to single MnO_x or CoO_x, and its surface oxygen was more effective in activating gaseous oxygen. The combination of manganese and cobalt enhanced the catalyst's redox characteristics and led to an increase in Lewis's acid sites. High oxygen mobility and rapid electron transport could keep highly valent metal ion and chemisorbed oxygen concentrations stable in the redox cycle ($Mn^{3+} + Co^{3+} \rightarrow Mn^{4+} + Co^{2+}$), speeding up the processing rate. Numerous defect sites would result from co-doping into MnO_x, which would facilitate the production of surface reactive oxygen species and improve NH_3 adsorption and activation in the SCR reaction. N_2O formation decreased, and N_2 selectivity was increased due to the electron transfer from Sm^{2+} to Mn^{4+}, which also prevented more $–NH_2$ dehydrogenation from generating –NH. Furthermore, adding Sm increased the likelihood that the initial N-H bond in NH_3 would break to cause $-NH_2$, speeding up the reaction rate. [49,50]

2.3.2.2.3. Supported manganese oxide-based catalysts

Support is one of the key factors influencing a catalyst's activity. The development and application of mixed metal oxides were restricted due to their small specific surface area, low dispersity, and other weaknesses despite their superior catalytic activity compared to single metal catalysts. Supported metal oxides have received much research attention to enhance catalyst performance even more. To prevent agglomeration-related catalytic performance

deterioration, the carrier promoted the active component's dispersity and supplied active sites. Supported metal oxides improved the redox performance and surface acidity of MnO_x-based catalysts, increased their dispersity, and improved electron transport between the active components due to the interaction between the metal components and the carrier. Carriers can be classified as reducible or irreducible based on their chemical structure. Usually, multivalent metal oxides like TiO_2, CeO_2, etc. were reducible supports. Numerous oxygen vacancies were supplied to the catalysts by the reducible carriers. To produce more fluid active oxygen species that could swiftly overflow to the surface of the active components and take part in SCR processes, they could sustainably absorb O_2 in the air. Usually, irreducible supports were non-variable valent oxides like SiO_2, Al_2O_3, etc. The excellent distribution of the active components was facilitated by the irreducible carrier's large specific surface area and pore structure. The catalysts' activity, stability, and usefulness were all greatly enhanced.

MnO_x-based catalysts supported on TiO_2

TiO_2 facilitates the even dispersion of the active components and provides NH_3 with an abundance of Lewis acid sites for adsorption. The formation of a TiO_2 shell layer on the surface of Mn–Fe nanotubes allowed for a longer period for the reaction gas to meet the catalyst, which increased the reactants' ability to adsorb on the catalyst surface. As a result, the catalytic performance of MnFe@TiO_2 was significantly higher than that of the Mn–Fe catalyst. Furthermore, increased Mn^{4+}, Fe^{3+}, and chemisorbed oxygen species may be produced by the combined action of the MnO_x, FeO_x, and TiO_2 shell layers. This could encourage the oxidation of NO to NO_2 and accelerate the fast-SCR reaction. Compared to conventional Mn/TiO_2 nanoparticles, Song et al. [50] confined MnO_2 in microporous TiO_2 with smaller molecular size, allowing the active intermediate NH_4NO_3 to be restricted and remain stable in small voids. This prevented the intermediates from directly breaking down to produce N_2O and greatly increased the selectivity of N_2. Using anatase TiO_2 particles of varying sizes as the support

material, Yang et al. [51] found that the MnO_x/TiO_2 (10–25) catalyst had the best SCR activity at low temperatures.

Multi-active component supported Mn–M/TiO_2 catalysts can further increase the SCR activity in comparison to single-active component MnO_2/TiO_2 catalysts. The same ratios of Ce, Fe, Co, and Ni were added to Mn/TiO_2 by Xie et al. [52], and this greatly increased the rate of NO conversion on M-Mn/TiO_2. The reason behind this was identified as the twin redox cycles (Mn^{4+} + M(n−1) + ← Mn^{3+} + Mn^{+}, Mn^{4+} + Ti^{3+} ← Mn^{3+} + Ti^{4+}) [53], which enhanced the catalyst's reducibility and produced additional Ti^{3+}, Mn^{4+}, and O_β.

MnO_x-Based catalysts supported on Al_2O_3

The Al_2O_3 support has a high porosity and large surface area, which enhances the cooperative action between the support and the active components and facilitates free electron migration. To increase the active components' dispersity on Mn/γ-Al_2O_3, Yang et al. [54] introduced Mo to the mixture. Additionally, Mo modification might result in the formation of more Mn^{3+} on the Al_2O_3 carrier surface, as well as more NH_3 being adsorbed on Mn^{n+} to undergo oxidative dehydrogenation and generate $–NH_2$ species, which would speed up the reactions. According to Yang et al. [55], at 150–200°C, NO conversion on the Fe–Mn/Al_2O_3 catalyst was higher than 95%. The TiO_2-Al_2O_3 composite support was prepared by Li et al. [56] using a coprecipitation method, which not only addressed the issue of the active components of the single TiO_2-supported catalyst efficiently aggregating but also significantly improved the surface acidity of the single Al_2O_3 supported MnO_x-based catalyst. Compared to the $MnCeO_x/Al_2O_3$ catalyst supported by a single Al_2O_3, the $MnCeO_x/TiO_2$-Al_2O_3 catalyst that was obtained showed higher activity and stability.

MnO_x-Based catalysts supported on carbon materials

Carbon materials offer excellent porosity, higher chemical stability, and tremendous surface areas such as carbon nanotubes (CNTs) and activated carbon (AC). In the catalytic process, they can supply many acid sites. In addition to improving the local concentration of metal

particles and internal reactants inside CNTs through a narrow space, using CNT materials as supports offered an excellent reaction site for the catalytic reaction. This also helped to improve the interaction between the internal surface of CNTs and the active metal phase. [57,58] To enhance the loading capacity and dispersion of metal oxides on the CNT carrier, Wang et al. [59] treated carbon nanotubes with nitric acid for an extended period, thereby increasing the amount of oxygen functional groups. This supported the previously mentioned views. An Mn-Ce-Fe/AC catalyst was synthesized by Yang et al. [60] using an impregnation technique. The average valence state of manganese ions was raised by Fe doping, which also enhanced oxygen mobility during the SCR process and the amount of NH3 that could be adsorbed on the activated carbon surface by exposing more acid-active sites [61]. The oxidation of NO to NO_2 may be facilitated by the redox cycling between the higher and lower valence states of Mn^{+}, increasing activity at low temperatures.

2.3.2.3. Ceria based catalysts

The CeO_2 nanocrystal contains a face-centered cubic (FCC) unit cell of cations with anions providing the octahedral interstitial sites. Its fluorite crystal structure has a lattice constant of a = 5.41134 Å. **Fig. 2.2**. shows the face-centered crystal cell of the CeO_2 structure. Four nearest-neighbor cerium cations and eight nearest-neighbor oxygen anions coordinate each oxygen anion, whereas eight cerium cations coordinate each. The generation of oxygen vacancies is the primary flaw in CeO_2 nanocrystals. Since all the oxygen atoms in the fluorite structure are in a plane with one another, diffusion can happen quickly depending on the quantity of oxygen vacancies. The subsequent defect reaction can result in a generation of oxygen vacancies:

$$2Ce_{ce} + O_o \rightarrow \frac{1}{2} O_2 + Vo + 2Ce'_{ce} \qquad [2.6]$$

where Ce_{ce} denotes Ce^{4+} in cerium lattice, O_o represents oxygen in oxygen lattice, Vo indicates oxygen vacancy and Ce'_{ce} signifies Ce^{3+} in cerium lattice.

The unique properties of CeO_2 primarily originate from the quick and reversible redox cycle between Ce^{4+} and Ce^{3+} in the fluorite lattice, through which the oxygen in gas phase can easily transfer into the solid surface where the chemical reaction occurs. CeO_2 has been considered as an excellent oxygen buffer, commonly defined in terms of oxygen storage capacity (OSC). As an excellent oxygen buffer, nano CeO_2 possesses three low index facets, including {111}, {110} and {100} surface. It is well known that exposed facet will lead to different atomic arrangement and coordination environment, affecting the physiochemical properties of ceria and ultimately its catalytic performance. [62,63]

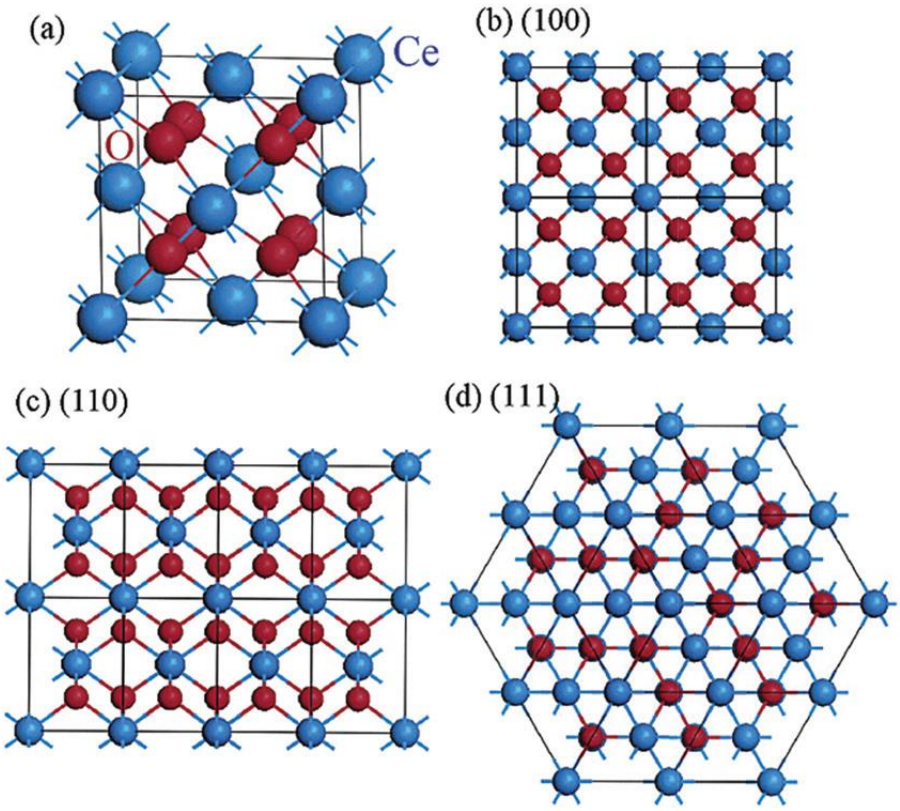

Fig. 2.2. (a) Crystal structure of ceria (b-d) (100), (110) and (111) planes of the ceria structure

Table 2.4. Review on Ceria based catalysts in NH_3-SCR studies

Catalysts	Reactant conditions

Preparation Techniques	Temperature window	Remarks	Ref.
CeO_2 (Hydrothermal and precipitation methods)	NO=500 ppm NH_3=500 ppm O_2=2% GHSV=5.0 × 10^4 h^{-1} (150-500°C)	The CeO_2-SH catalyst gave >97% NO_x conversion between the 230-450°C, and showed excellent resistance to Na and K.	[64]
Ce-P-O (Hydrothermal method)	NO=1000 ppm NH_3=1000 ppm O_2=10 % GHSV=20 000 h^{-1} (100-600°C)	The Ce-P-O catalyst exhibits excellent deNO_x activity and resistance to K_2O and SO_2/H_2O in wide temperature range.	[65]
CeO_2-TiO_2 (Sol–gel method)	NO=1000 ppm O_2=3 vol.% Flow rate=500 ml-min^{-1} (150-450°C)	The CeO_2/TiO_2 catalyst with mass ratio of 0.6, showed the highest (more than 90%) NO conversion between 250-450 °C and showed excellent tolerance to SO_2 and H_2O.	[68]
Mn-Ce-Ti (Hydrothermal method)	NO=500 ppm NH_3=500 ppm O_2=5% GHSV =64 000 h^{-1} (100-400°C)	Mn-Ce-Ti mixed-oxide catalyst exhibited NO_x *(*>90%*)* in a wide temperature range (150-350°C) and was highly resistant against H_2O and SO_2.	[69]
CuO–CeO_2–TiO_2 (Sol-gel method)	NO=500 ppm NH_3= 500 ppm O_2=5% GHSV= 30 000 h^{-1} (100-350°C)	CuO-CeO_2–TiO_2 catalyst showed the highest NH_3-SCR activity (>80%) in a low-temperature range of 150–250°C.	[70]
Fe–Ce/TiO_2 (Impregnation method)	NO=1000 ppm NH_3=1000 ppm O_2= 3 vol % GHSV=30 000 h^{-1} (0-300°C)	At the 160 °C, the Fe-Ce/TiO_2 catalyst (molar ratio of 0.2) gave 80% NO_x conversion. With 500 ppm SO_2, the Fe-Ce/TiO_2 catalyst gave 94% NO_x conversion at 250°C.	[71]

CeO_2/CNTs (Pyridine-thermal route)	NO= 500 ppm NH_3= 500 ppm O_2= 3 vol% GHSV =20 000 h^{-1} (150 -380°C)	The CeO_2/CNTs catalyst gave the >90% NO conversion, and desirable N_2 selectivity in the 250-370°C temperature range. The NO conversion was 97% with SO_2 or H_2O at 300°C.	[72]

Many studies on ceria-based catalysts for NH_3-SCR have been performed in recent years, which is summarized in **Table 2.4**. According to its existence and mode of use, ceria in catalysts can generally be divided into three categories: bulk doping, surface modification, and usage as a pure support or active component in a "surface to bulk" sequence.

2.3.2.3.1. Pure CeO_2 as an active component or support

In general, pure CeO_2 has weak NH_3-SCR activity. Guo et al. [66] investigated the effects of calcination temperature and precursor. They found 80% NO conversion at 250°C. Tang et al. [67] prepared CeO_2 via a controlled thermal decomposition of cerium oxalate. They found that the best activity reached 100% NO conversion at the temperature range of 275–425°C. Li and co-workers [64] prepared a series of ceria catalysts using sulphate and nitrate precursors by hydrothermal and precipitation methods. Among them, the CeO_2 catalyst prepared by hydrothermal method with cerium (IV) sulphate as a precursor showed excellent SCR activity and high N_2 selectivity in the temperature range of 230–450°C. Yang et al. [65] used pyrophosphoric acid and hydrothermal treatment to synthesize ceria from cerium nitrate. The enhanced acidity brought about by the sulphate and polyphosphate ions was identified as the cause of the activity boost in these two situations.

To further improve the activity of ceria, researchers have used ceria as support to deposit active components. In this case, ceria may influence the electrical and redox characteristics of surface-dispersed species and act as a disperser of active species. It is also possible that some synergy will occur at the interfacial region, which will ultimately add to the outstanding results. Xu et

al. [73] deposited MnO_x onto CeO_2 with a deposition-precipitation (DP) method and found nearly 100% NO conversion between 80-150°C. With further investigations, researchers will explore CeO_2-supported dual or even multiple metal-oxide catalysts. Zhu et al. [74] synthesized a series of ceria-supported bimetallic oxide (Ni–Mo, Cu–Ni, and Fe–Mo) catalysts and investigated their catalytic performance in NH_3-SCR. Incorporating NiO, CuO, and Fe_2O_3 into MoO_3/CeO_2, catalysts yielded varied surface molybdenum structures-isolated regular tetrahedral, highly distorted tetrahedral, and polymerized octahedral forms. Interaction strengths between molybdenum species and these metal oxides mirrored the Lewis acid site acidities, indicating strong reactivity dependence on catalyst acidity.

2.3.2.3.2. Ceria-based mixed oxides

Ceria-based mixed oxide catalysts are more commonly used for NH_3-SCR. Enhancing the catalytic performance and thermal stability of CeO_2 usually involves bulk modification. By adding suitable oxides, CeO_2's characteristics can be changed to generate spinel, binary or multivariate solid solutions, perovskite oxides, or mixed oxides. One metal element in a composite oxide catalyst can change another's catalytic characteristics due to structural and electrical effects. It is possible to apply this composite oxide directly as catalysts (CeO_2-TiO_2, CeO_2-MnO_x), which are becoming more and more appealing because of their high activity, or as a support following bulk modification of CeO_2 (CeO_2-ZrO_2, CeO_2-SnO_2). Qi et al. [75] synthesized MnO_x–CeO_2 catalysts. The results show that in the low-temperature window of 80–150 °C with 100% N_2 selectivity and complete NO conversion at temperatures at 120°C. Gao et al. [68] synthesized Ce–Ti mixed-oxide catalysts through the sol-gel method. The CeO_2/TiO_2 mass ratio of 0.6 provided the highest active catalyst.

The ceria-based mixed oxide catalysts with multiple components were anaylzed and showed effective ways to enhance the activity and extend the temperature window of catalysts in NH_3-SCR. Liu et al. [76] synthesized Cu-Ce-Ti oxide by a hydrothermal method and found that the

ternary component catalysts displayed much better activity than the binary Cu-Ti and Ce-Ti oxide catalysts. The results show that $Cu_{0.1}Ce_{0.1}Ti_{0.8}O_x$, with more than 70% NO conversion at 150 °C and nearly 100% conversion between 200 and 350°C. A similar effect was also observed for the Mn-Ce-Ti oxide system.[69] According to Chen et al.'s analysis [70], the CuO-CeO_2-TiO_2 ternary oxide catalyst exhibited excellent NH_3-SCR activity in the 150-250°C low-temperature range.

The preparation methods are also an important factor that influences the activity of catalysts. The common methods used to synthesize composite oxide catalysts are co-precipitation, hydrothermal, citric acid method, sol–gel, and homogeneous precipitation. Shan et al. [77] synthesized the $CeTiO_x$ mixed oxide catalyst through homogeneous precipitation. The catalyst showed much higher NH_3-SCR activity than the supported CeO_2/TiO_2 catalyst, with significantly improved resistance to high space velocity. Gao et al. [78] synthesized CeO_2–TiO_2 catalysts by three methods, and the results showed that the catalyst prepared by a single-step sol–gel method had the highest NH_3-SCR activity. The strong interaction between Ce and Ti, along with the high concentration of amorphous or highly dispersed nano-crystalline ceria, could be responsible for the excellent performance of the catalyst generated by the single-step sol–gel method. Increased surface area and good redox properties enhanced the catalytic activity. Liu et al. [79] synthesized cerium–tungsten oxide by impregnation and solid processing methods and showed better NH_3-SCR activity than those prepared via the sol-gel method in the 175–500°C temperature range.

2.3.2.3.3. CeO_2 as surface loading component (surface modification)

Carriers like TiO_2, Al_2O_3, and SiO_2 have been used to support ceria for low-temperature NH_3-SCR. Among them, TiO_2 is most widely reported because of its nontoxicity, biological and

chemical inertness, poor interaction with SO_2, and easy availability. Xu et al. [80] synthesized a CeO_2/TiO_2 catalyst using impregnation method. The temperature range of 275–400°C showed high activity and good N_2 selectivity. Wang et al. [81] introduced CeO_2 into the tubular channels of titanium nanotubes (TNTs). The superior NH_3-SCR performance of the confined ceria was attributed to their unique NH_3 adsorption and enhanced redox potential when compared to catalysts supported by TiO_2 nanoparticles. Additionally, they synthesized two catalysts by depositing ceria nanoparticles both inside and outside of TNTs. [82] CeO_2 catalyst contained in titanate nanotubes exhibited exceptional resistance to alkali metal toxicity. Shu et al. [71] investigated the effect of iron additives on the catalytic performance of the CeO_2/TiO_2 and found that iron could enhance the low-temperature activity and SO_2-poisoning resistance of the CeO_2/TiO_2 catalyst.

Carbon materials have also been used as supports for NH_3-SCR reactions with high surface area and pore volume, resulting in highly dispersed active sites. It is necessary to pre-activate carbon materials to improve their catalytic performance. Fang et al. [72] used a pyridine-thermal route to disperse CeO_2 on CNTs. Pyrididine-thermal catalysts are more effective than impregnated or physical mixture catalysts for NH_3-SCR. Due to its special characteristics, activated carbon fiber can also be used as a catalyst for removing pollution sources. Lu et al. [83] studied the catalytic stability of 10–40% CeO_2/ACF at 200°C and the catalytic activity at different temperatures. The results show that 10% CeO_2/ACF can convert NO and maintain higher catalytic activity at higher temperatures.

Zeolites have received much attention in recent years due to their enriched acidity and thermal stability, and many metal-ions exchanged zeolites such as Fe/SSZ-13, Cu/SAPO-34, Mn/NaY, and Ce/ZSM-5 are active in the NH_3-SCR reaction. Recently, SCR catalysts based on chabazite-type zeolites (e.g., SSZ-13, SAPO-34) with improved activities and high thermal durability have been reported for NH_3-SCR. Iron and copper zeolites are among the most

intriguing and well-researched members of this large class of catalysts. On the other hand, there weren't many reports of ceria being supported on zeolites as an active component. This is explained by two factors: the likelihood of producing CeO_2 segregates that emerge as clusters after calcination and the decrease in the degree of crystallinity of Ce-exchanged zeolites during the exchange process. Ce-zeolite catalysts for SCR of NO_x with NH_3 were generally prepared by aqueous ion exchange (IE) procedure, and obtaining a high ion exchange percentage of Ce^{3+} is impossible. IE of Ce^{3+} often results in CeO_2 along with other cations in the zeolite, which affects the catalytic activity. Kooten et al. [84] synthesized Ce–NaZSM-5 catalysts through the solid-state ion exchange, which showed excellent NO_x conversion in NH_3-SCR.

2.3.3. Zeolite based catalysts

In last decade, zeolite-based catalysts with unique pore structures and excellent catalytic performance have attracted increasing attention and application in petrochemical and environmental fields. Metal-exchanged small-pore zeolites are the most effective catalysts for the removal of NO_x and are high-efficiency substitute of traditional V_2O_5/TiO_2 catalysts. In recent years, Cu-based exchanged zeolites have been the most widely studied zeolite catalyst in NO_x removal in the wide temperature window.

Table 2.5. Review on zeolite-based catalysts in NH_3-SCR studies

Catalysts	**Feed gas conditions**		
Preparation Techniques	**Temperature window**	**Remarks**	**Ref.**

Mn-ZSM-5 (Hydrothermal methods)	NO=400 ppmv NH_3 = 400 ppmv O_2=6vol.% GHSV=1.4 x10^4 h^{-1} (100–450°C)	The results reveal that, across the temperature range of 100-400°C, Mn-ZSM has provided the maximum NO_x conversion (<90%).	[86]
Cu–SSZ-39 (Hydrothermal methods)	NO=NH_3=500 ppm O_2=7vol.% GHSV=27 000 h^{-1} (100-550°C)	Showing NO_x conversions close to 100% up to 350°C, and >85% NO_x conversion at 450°C.	[87]
Fe/Mn-SBA-15 (Impregnation method)	NO=300 ppm NH_3=300 ppm O_2= 3 vol% GHSV=120,000 h^{-1} (100–350°C)	The results shows that the Fe-Mn/SBA-15 catalyst shows synergistic effect between Fe and Mn and gave more than 90% NO_x conversion in the 200–250°C temperature range.	[88]
CuFe-SSZ-13 (Solid-state ion-exchange method, Homogeneous deposition precipitation method)	NO=500 ppm NH_3=500 ppm O_2= 5% GHSV=400,000 h^{-1} (100-550°C)	The CuFe-SSZ-13 catalyst synthesis through the Homogeneous deposition precipitation method showed the best NO_x conversion (<90%) compared the other methods in the temperature range of 100-550°C	[89]
Cu-SAPO-34 (Cu-CZC), Fe-Mordenite (Fe-MOR) (Ion exchange)	NO, NO_2=75ppm NH_3=150ppm O_2=10% GHSV=143 076 h^{-1} (150-450°C)	Cu-CZC showed high NO_x activity at lower temperatures (75% of NO_x conversion at T < 300 °C), while Fe-MOR was more active (>85%) at higher temperatures (300–450°C).	[90]
Cu–Mn/ZSM-5, Cu–Mn/SAPO-34 (Liquid ion exchange method)	NO=300 ppm NH_3= 300 ppm O_2= 14% GHSV=30 000 h^{-1} (100-500°C)	The NO_x conversions on Cu–Mn/ZSM-5 and Cu–Mn/SAPO-34 at 200°C were 65% and 90%, respectively, at a Cu/Mn ratio 3:2.	[91]

Based on the number of atoms (T) in the ring, zeolites can be categorized as eight-member rings (LTA, GIS, CHA, AEI), ten-member rings (MFI), twelve-member rings (FAU, MOR, BEA), and ultra-large pore zeolites (where the number of T in the pore is greater than 12). [85] Most zeolites have suitable surface acidity, flexibility and good adsorption properties which results in high hydrothermal stability and tolerance to poisoning. The different zeolite-based catalysts in NH_3-SCR studies have been summarized in the **Table 2.5**.

To improve NH_3-SCR performance in the zeolite-based catalysts are modified with single metals like Cu, Fe, and Mn to achieve excellent denitrification efficiency, N_2 selectivity, and hydrothermal stability. Fan et al. [92] synthesized Cu-SSZ-13 catalysts for the low temperature's performance and results revealed that at low temperatures (< 250°C), NO conversion was above 87%. Furthermore, the loss of some isolated Cu^{2+} ions and the hydrothermally treated catalyst's surface acidity explained the drop-in catalytic activity below 250°C than between 250 and 475°C.

2.3.4. Perovskite catalysts

Perovskite oxides have attracted significant interest because of their excellent structural stability, high catalytic activity, and modifiable electronic properties. In an ABO_3 structure, lattice defects and oxygen vacancies occur when partial replacement of A ions occurs by other ions; resulting in change in the valence states of B ions to maintain balance. The catalytic activity in perovskites catalyst is associated to these vacancies and defects. The different Perovskite based catalysts in NH_3-SCR studies have been summarized in the **Table 2.6**.

Table 2.6. Review on perovskite catalysts in NH_3-SCR studies

Catalysts	**Feed gas conditions**	**Remarks**	**Ref.**
Preparation Techniques	**Temperature window**		

Ce modified La-Mn (Sol-gel method)	NO=500 ppm NH_3= 500 ppm O_2= 5 vol.% GHSV=30,000 h^{-1} (80-300°C)	The catalyst showed best SCR activity at a Ce/Mn ratio of 0.2, obtaining 90% NO_x conversion at 135°C and more than 70% N_2 selectivity. In the presence of SO_2 and H_2O, 95% NO_x conversion was achieved at 200°C	[93]
Mn doped perovskite La-Mn oxides (Sol–gel method)	NO=500 ppm NH_3= 500 ppm O_2= 5 vol% GHSV=30,000 h^{-1} (80~300°C)	The La-Mn-1.4 catalyst gave 80% NO_x conversion at 100–300°C. In the presence of SO_2 and H_2O, the LM-1.4 gave 95% NO_x conversion and excellent N_2 selectivity	[94]
$LaMnO_3$/biochar (Sol-gel method)	NO=500 ppm NH_3=500 ppm O_2= 5 vol % GHSV=16 000 h^{-1} (100-250°C)	The $LaMnO_3$/biochar catalyst showed excellent performance and achieved over 90% NO conversion and N_2 selectivity in the 100–250°C temperature range. The highest NO conversion of 95% was obtained at 225°C.	[95]
$Pr_{1-x}Ce_xCo_{0.5}Mn_{0.5}O_3$ (Glucose complex method)	NO=1000 ppm NH_3= 1000 ppm O_2= 5% GHSV=20,000 h^{-1} (0–600ºC)	The results showed the porous structure and the excellent low-temperature redox performance of the $Pr_{0.8}Ce_{0.2}Co_{0.5}Mn_{0.5}O_3$ catalyst. The NO_x conversion was 90% at 400°C.	[96]
Ni-MOF (Solvothermal method)	NO=500 ppm O_2 NH_3=500 ppm NH_3 O_2= 5 vol% GHSV=15,000 h^{-1} (100 -500°C)	Preheating treatment with the N_2 improved the catalytic activity of the Ni-MOF catalyst. Activation at 220°C results in 92% NO conversion in the wide range of 275- 440°C	[97]
CuMgAl-LDH (Coprecipitation method)	NO=600 ppm NH_3= 600 ppm O_2= 5.0 vol% GHSV = 45,000h^{-1} (90-330°C)	The CuMgAl-SDSO-LDO catalyst demonstrated higher dispersion and more suitable valence state distribution of Cu. It showed 90% NO_x conversion at 210°C and 75% N_2 selectivity and excellent H_2O/SO_2 resistance	[98]

In the research work, Shi et al. [93] synthesized Ce-doped La-Mn perovskite catalysts through the sol-gel method and observed that Ce/Mn ratio of 0.2 is favourable for the SCR activity. At 200°C, in presence of SO_2 and H_2O, it achieved 95% NO_x conversion and more than 70% N_2 selectivity. Compared to the undoped sample for the de-NO_x performance, the Ce-doped La-Mn perovskite catalysts offered higher specific surface area, more acidic sites, more chemically adsorbed oxygen and improved redox performance. The results revealed that the LM-1.4 catalyst worked in a wide window temperature (80% NO_x conversion in 100–300°C).

Fan et al. [95] synthesized a biochar-supported perovskite oxide catalyst and resulted in 80% NO conversion in the 100-250°C temperature range by the $LaMnO_3$/biochar catalyst. The maximum NO conversion was 95.8% at 225°C (SN_2 = 95.4%). Due to the acidic function of the perovskite oxide and the acidic oxygen-containing functional groups of the modified biochar substrate, the catalyst offered synergistic adsorption of the capacity for NH_3. Nie et al. [96] synthesized $Pr_{1-x}Ce_xCo_{0.5}Mn_{0.5}O_3$ catalysts through the glucose complexation method with elements Pr, Ce, Mn, and Co. The catalyst $Pr_{0.8}Ce_{0.2}Co_{0.5}Mn_{0.5}O_3$ demonstrated a porous structure and outstanding low-temperature redox capability, as evidenced by the catalyst's 90% conversion rate at 400°C. The catalyst was impregnated on the cordierite honeycomb ceramic support and converted NO_x up to 95% at 350°C. Sun et al. [97] fabricated Ni-MOF catalysts through the hydrothermal method. The Ni-MOF displayed more thermally stable behaviour than Cu-BTC or MIL-100(Fe) SCR catalysts. When the reaction temperature reaches 440°C, it retains a satisfactory, stable crystal structure. Preheating Ni-MOF with the N_2 improved its catalytic activity significantly. More than 92% of NO conversion was found for the Ni-MOF catalyst activated at 220°C with a large operating temperature window of 275 to 440°C. Wu et al. [98] synthesized sodium dodecyl sulfonate (SDSO) intercalated CuMgAl Layered double hydroxide (CuMgAl-SDSO-LDH) catalyst. The denitrification activity of CuMgAl-NO_3-LDO

was found to be influenced by the existence of carbon from SDSO. The results of the characterization analysis showed that the CuMgAl-SDSO-LDO catalyst performed best when the dispersion and valence state distribution of Cu were higher. These factors were intrinsically related to the moderate carbon doping content and resulted in excellent SCR performance, with 90% NO_x conversion at 210°C and strong H_2O/SO_2 resistance ability.

2.4. Conclusions from literature

Many studies have focused on $V_2O_5–WO_3(MoO_3)/TiO_2$ catalysts commercially applied in thermal power plants because of the high NO_x removal efficiency at 300–400°C. Moreover, the traditional V-based catalysts are not applicable in steel, cement, and glass plants due to low-temperature of flue gas (<250°C). The deposition of $(NH_4)_2SO_4/NH_4HSO_4$ and metal sulphates becomes more serious in low temperature ranges which blocks and destroy the active sites, respectively. From academic and industrial viewpoints, new types of SCR catalysts should be qualified with the following characteristics: broad operating window, high SO_2/H_2O-tolerance at low temperatures, highly alkali/heavy metal/P/HCl-resistant ability, strong hydrothermal stability. Developing efficient MnO_x-based catalysts for low-temperature NH_3-SCR has received considerable attention due to their variable oxidation states and crystal structures. Furthermore, catalysis systems based on MnO_x supported on various transition metal oxides (TiO_2, Al_2O_3, CeO_2, and ZrO_2) have shown high performance for low-temperature SCR catalysts. CeO_2 as a catalyst support or mixed oxide has attracted great attention due to its redox and high oxygen storage properties. Among the various metallic oxides, MnO_x-CeO_2 catalysts have shown a lot of potential because of the high oxygen storage capacity of CeO_2. The reaction mechanism of NH_3-SCR of NO_x is strongly influenced by the active metal's support and nature (MnO_x) and is also affected by the reaction conditions.

2.5. Purpose of present work

A vast amount of literature is available describing the conversion and selectivity of various combinations of metal catalyst, support, and reducing agent. However, much less attention has been paid to the optimization of the structure and oxidation state of the active catalysts, its advancement under reaction conditions and its influence on catalytic performance.

Cerium oxide, or ceria (CeO_2), has inspired the scientific community's interest for decades due to its applications in a variety of catalytic areas, including three-way catalytic converters (TWCs), soot removal from diesel engine exhaust and fuel cell technology. CeO_2 nanomaterials have grabbed interest due to their high oxygen storage capacity and a unique Ce^{4+}/Ce^{3+} redox cycle that enhances reactant activation on the ceria surface. CeO_2's oxygen storage component allows the catalysts to operate at higher air-to-fuel ratios. Pure CeO_2 nanoparticles are unable to meet the standards for practical usage due to their poor thermal stability and susceptibility to SO_2, restricting their practical application. In most cases, combining CeO_2 with transition metal oxides improves catalytic activity because of their low cost and outstanding redox characteristics. The present work focuses on the reduction of NO using NH_3 as oxidant. This reaction has potential technological applications due to its lower onset temperature and high NO_x removal efficiency. The present study focused on to maximize the dispersion of active metal over support and efficacy of the catalysts for low temperature SCR reaction.

References

1. Graus, W.H.J. and Worrell, E., 2007. Effects of SO_2 and NO_x control on energy-efficiency power generation. *Energy Policy*, *35*(7), pp.3898-3908.
2. Cai, T., Zhao, D., Sun, Y., Ni, S., Li, W., Guan, D. and Wang, B., 2021. Evaluation of NO_x emissions characteristics in a CO_2-Free micro-power system by implementing a perforated plate. *Renewable and Sustainable Energy Reviews*, *145*, p.111150.

3. ZHANG, W.B., CHEN, J.L., Li, G.U.O., ZHENG, W., WANG, G.H., ZHENG, S.K. and WU, X.Q., 2021. Research progress on NH_3-SCR mechanism of metal-supported zeolite catalysts. *Journal of Fuel Chemistry and Technology*, *49*(9), pp.1294-1315.
4. Zhang, M., Guan, Z., Qiao, Y., Zhou, S., Chen, G., Guo, R., Pan, W., Wu, J., Li, F. and Ren, J., 2024. The impact of catalyst structure and morphology on the catalytic performance in NH_3-SCR reaction: A review. *Fuel*, *361*, p.130541.
5. Baik, J.H., Yim, S.D., Nam, I.S., Mok, Y.S., Lee, J.H., Cho, B.K. and Oh, S.H., 2004. Control of NO_x emissions from diesel engine by selective catalytic reduction (SCR) with urea. *Topics in catalysis*, *30*, pp.37-41.
6. Khatri, P. and Bhatia, D., 2023. Influence of catalyst composition on NO_x storage and reduction characteristics of Ag catalyst supported on MgO-doped alumina. *Chemical Engineering Research and Design*, *197*, pp.476-495.
7. Cao, F., Xiang, J., Su, S., Wang, P., Hu, S. and Sun, L., 2015. Ag modified Mn–Ce/γ-Al_2O_3 catalyst for selective catalytic reduction of NO with NH_3 at low-temperature. *Fuel Processing Technology*, *135*, pp.66-72.
8. Perumal, S.K., Kaisare, N., Kummari, S.K. and Aghalayam, P., 2022. Low-temperature NH_3-SCR of NO over robust RuNi/Al-SBA-15 catalysts: Effect of Ru loading. *Journal of Environmental Chemical Engineering*, *10*(5), p.108288.
9. Ren, Z., Zhang, H., Wang, G., Pan, Y., Yu, Z. and Long, H., 2020. Effect of Calcination Temperature on the Activation Performance and Reaction Mechanism of Ce–Mn–Ru/TiO_2 Catalysts for Selective Catalytic Reduction of NO with NH_3. *ACS omega*, *5*(51), pp.33357-33371.
10. Wei, F., Rao, Y., Huang, Y., Wang, W. and Mei, H., 2023. The new challenges for the development of NH_3-SCR catalysts under new situation of energy transition in power generation industry. *Chinese Chemical Letters*, p.108931.

11. Zhang, K., Luo, N., Huang, Z., Zhao, G., Chu, F., Yang, R., Tang, X., Wang, G., Gao, F. and Huang, X., 2023. Recent advances in low-temperature NH_3-SCR of NO_x over Ce-based catalysts: Performance optimizations, reaction mechanisms and anti-poisoning countermeasures. *Chemical Engineering Journal*, *476*, p.146889.
12. Yan, Z., Shan, W., Shi, X., He, G., Lian, Z., Yu, Y., Shan, Y., Liu, J. and He, H., 2020. The way to enhance the thermal stability of V_2O_5-based catalysts for NH_3-SCR. *Catalysis Today*, *355*, pp.408-414.
13. Zhang, P. and Li, D., 2014. Selective catalytic reduction of NO with NH_3 over iron–vanadium mixed oxide catalyst. *Catalysis letters*, *144*, pp.959-963.
14. Koh, H.L., Lee, S.H. and Kim, K.L., 2000. The effect of MoO_3 addition to V_2O_5/Al_2O_3 catalysts for the selective catalytic reduction of NO by NH_3. *Reaction Kinetics and Catalysis Letters*, *71*, pp.239-244.
15. Wu, R., Li, L., Zhang, N., He, J., Song, L., Zhang, G., Zhang, Z. and He, H., 2021. Enhancement of low-temperature NH_3-SCR catalytic activity and H_2O & SO_2 resistance over commercial V_2O_5-MoO_3/TiO_2 catalyst by high shear-induced doping of expanded graphite. *Catalysis Today*, *376*, pp.302-310.
16. Qi, L., Li, S., Wang, W. and Li, J., 2023. Investigation of Mg-doping effect on the activity and P tolerance of V_2O_5-MoO_3/TiO_2 catalysts for NH_3-SCR. *Environmental Science and Pollution Research*, *30*(22), pp.62880-62891.
17. Zhang, P. and Li, D., 2014. Selective catalytic reduction of NO with NH_3 over iron-vanadium mixed oxide catalyst. *Catalysis letters*, *144*, pp.959-963.
18. Chen, T., Lin, H., Guan, B., Gong, X., Li, K. and Huang, Z., 2016. Promoting the low temperature activity of Ti–V–O catalysts by premixed flame synthesis. *Chemical Engineering Journal*, *296*, pp.45-55.

19. Soh, B.W., Nam, I.S. and Lee, J.B., 1999. Morphological impact of V_2O_5/Al_2O_3 catalyst on the deactivation by SO_2 for the reduction of NO with NH_3. In *Studies in Surface Science and Catalysis* (Vol. 126, pp. 389-396). Elsevier.
20. Boyano, A., Lázaro, M.J., Cristiani, C., Maldonado-Hodar, F.J., Forzatti, P. and Moliner, R., 2009. A comparative study of V_2O_5/AC and V_2O_5/Al_2O_3 catalysts for the selective catalytic reduction of NO by NH_3. *Chemical Engineering Journal*, *149*(1-3), pp.173-182.
21. Huang, X., Zhang, S., Chen, H. and Zhong, Q., 2015. Selective catalytic reduction of NO with NH_3 over V_2O_5 supported on TiO_2 and Al_2O_3: A comparative study. *Journal of Molecular structure*, *1098*, pp.289-297.
22. Cha, W., Le, H.A., Chin, S., Kim, M., Jung, H., Yun, S.T. and Jurng, J., 2013. Enhanced low-temperature NH_3-SCR activity of a V_2O_5/TiO_2 composite prepared via chemical vapor condensation and impregnation method. *Materials Research Bulletin*, *48*(10), pp.4415-4418.
23. Giakoumelou, I., Fountzoula, C., Kordulis, C. and Boghosian, S., 2006. Molecular structure and catalytic activity of V_2O_5/TiO_2 catalysts for the SCR of NO by NH_3: In situ Raman spectra in the presence of O_2, NH_3, NO, H_2, H_2O, and SO_2. *Journal of Catalysis*, *239*(1), pp.1-12.
24. Huang, Z., Liu, Z., Zhang, X. and Liu, Q., 2006. Inhibition effect of H_2O on V_2O_5/AC catalyst for catalytic reduction of NO with NH_3 at low temperature. *Applied Catalysis B: Environmental*, *63*(3-4), pp.260-265.
25. Huang, Z., Zhu, Z. and Liu, Z., 2002. Combined effect of H_2O and SO_2 on V_2O_5/AC catalysts for NO reduction with ammonia at lower temperatures. *Applied Catalysis B: Environmental*, *39*(4), pp.361-368.

26. Bai, S., Jiang, S., Li, H. and Guan, Y., 2015. Carbon nanotubes loaded with vanadium oxide for reduction NO with NH_3 at low temperature. *Chinese Journal of Chemical Engineering*, *23*(3), pp.516-519.
27. BAI, S.L., ZHAO, J.H., Li, W.A.N.G. and ZHU, Z.P., 2009. Study of low-temperature selective catalytic reduction of NO by ammonia over carbon-nanotube-supported vanadium. *Journal of Fuel Chemistry and Technology*, *37*(5), pp.583-587.
28. Vuong, T.H., Radnik, J., Kondratenko, E., Schneider, M., Armbruster, U. and Brückner, A., 2016. Structure-reactivity relationships in $VO_x/Ce_xZr_{1-x}O_2$ catalysts used for low-temperature NH_3-SCR of NO. *Applied Catalysis B: Environmental*, *197*, pp.159-167.
29. Zhao, L., Li, C., Li, S., Wang, Y., Zhang, J., Wang, T. and Zeng, G., 2016. Simultaneous removal of elemental mercury and NO in simulated flue gas over V_2O_5/ZrO_2-CeO_2 catalyst. *Applied Catalysis B: Environmental*, *198*, pp.420-430.
30. Liu, C., Shi, J.W., Gao, C. and Niu, C., 2016. Manganese oxide-based catalysts for low-temperature selective catalytic reduction of NO_x with NH_3: A review. *Applied Catalysis A: General*, *522*, pp.54-69.
31. Takagi-Kawai, M., Soma, M., Onishi, T. and Tamaru, K., 1980. The adsorption and the reaction of NH_3 and NO_x on supported V_2O_5 catalysts: effect of supporting materials. *Canadian Journal of Chemistry*, *58*(20), pp.2132-2137.
32. Camposeco, R., Castillo, S., Mugica, V., Mejia-Centeno, I. and Marín, J., 2014. Novel $V_2O_5/NTiO_2–Al_2O_3$ nanostructured catalysts for enhanced catalytic activity in NO reduction by NH_3. *Catalysis Communications*, *45*, pp.54-58.
33. Tang, X., Hao, J., Xu, W. and Li, J., 2007. Low temperature selective catalytic reduction of NO_x with NH_3 over amorphous MnO_x catalysts prepared by three methods. *Catalysis Communications*, *8*(3), pp.329-334.

34. Kang, M., Yeon, T.H., Park, E.D., Yie, J.E. and Kim, J.M., 2006. Novel MnO_x catalysts for NO reduction at low temperature with ammonia. *Catalysis letters*, *106*, pp.77-80.
35. Gong, P., Xie, J., Fang, D., Han, D., He, F., Li, F. and Qi, K., 2017. Effects of surface physicochemical properties on NH_3-SCR activity of MnO_2 catalysts with different crystal structures. *Chinese Journal of Catalysis*, *38*(11), pp.1925-1934.
36. Zhang, C., Chen, T., Liu, H., Chen, D., Xu, B. and Qing, C., 2018. Low temperature SCR reaction over Nano-Structured Fe-Mn Oxides: Characterization, performance, and kinetic study. *Applied Surface Science*, *457*, pp.1116-1125.
37. Xie, H., Shu, D., Chen, T., Liu, H., Zou, X., Wang, C., Han, Z. and Chen, D., 2022. An in-situ DRIFTs study of Mn doped $FeVO_4$ catalyst by one-pot synthesis for low-temperature NH_3-SCR. *Fuel*, *309*, p.122108.
38. Tang, X., Wang, C., Gao, F., Zhang, R., Shi, Y. and Yi, H., 2021. Acid modification enhances selective catalytic reduction activity and sulphur dioxide resistance of manganese-cerium-cobalt catalysts: Insight into the role of phosphotungstic acid. *Journal of Colloid and Interface Science*, *603*, pp.291-306.
39. Huang, J., Huang, H., Jiang, H. and Liu, L., 2019. The promotional role of Nd on Mn/TiO_2 catalyst for the low-temperature NH_3-SCR of NO_x. *Catalysis Today*, *332*, pp.49-58.
40. Zhang, Q., Qiu, C., Xu, H., Lin, T., Lin, Z., Gong, M. and Chen, Y., 2011. Low-temperature selective catalytic reduction of NO with NH_3 over monolith catalyst of $MnO_x/CeO_2–ZrO_2–Al_2O_3$. *Catalysis Today*, *175*(1), pp.171-176.
41. Kapteijn, F., Singoredjo, L., Andreini, A. and Moulijn, J.A., 1994. Activity and selectivity of pure manganese oxides in the selective catalytic reduction of nitric oxide with ammonia. *Applied Catalysis B: Environmental*, *3*(2-3), pp.173-189.

42. Gong, P., Xie, J., Fang, D., Han, D., He, F., Li, F. and Qi, K., 2017. Effects of surface physicochemical properties on NH_3-SCR activity of MnO_2 catalysts with different crystal structures. *Chinese Journal of Catalysis*, *38*(11), pp.1925-1934.
43. Shao, J., Wang, Z., Liu, P., Lin, F., Zhu, Y., He, Y. and Cen, K., 2021. Interplay effect on simultaneous catalytic oxidation of NO_x and toluene over different crystal types of MnO_2 catalysts. *Proceedings of the Combustion Institute*, *38*(4), pp.5433-5441.
44. Liu, C., Wang, H., Zhang, Z. and Liu, Q., 2020. The latest research progress of NH_3-SCR in the SO_2 resistance of the catalyst in low temperatures for selective catalytic reduction of NO_x. *Catalysts*, *10*(9), p.1034.
45. Shi, J.W., Gao, C., Liu, C., Fan, Z., Gao, G. and Niu, C., 2017. Porous MnO_x for low-temperature NH_3-SCR of NO_x: the intrinsic relationship between surface physicochemical property and catalytic activity. *Journal of Nanoparticle Research*, *19*, pp.1-11.
46. Wang, Z.Y., Guo, R.T., Shi, X., Liu, X.Y., Qin, H., Liu, Y.Z., Duan, C.P., Guo, D.Y. and Pan, W.G., 2020. The superior performance of $CoMnO_x$ catalyst with ball-flowerlike structure for low-temperature selective catalytic reduction of NO_x by NH_3. *Chemical Engineering Journal*, *381*, p.122753.
47. Duan, C.P., Guo, R.T., Wu, G.L. and Pan, W.G., 2020. Selective catalytic reduction of NO_x by NH_3 over $CeVO_4$-CeO_2 nanocomposite. *Environmental Science and Pollution Research*, *27*, pp.22818-22828.
48. Zhang, X., Zhang, X., Yang, X., Chen, Y., Hu, X. and Wu, X., 2021. CeMn/TiO_2 catalysts prepared by different methods for enhanced low-temperature NH_3-SCR catalytic performance. *Chemical Engineering Science*, *238*, p.116588.

49. Liu, L., Xu, K., Su, S., He, L., Qing, M., Chi, H., Liu, T., Hu, S., Wang, Y. and Xiang, J., 2020. Efficient Sm modified Mn/TiO_2 catalysts for selective catalytic reduction of NO with NH_3 at low temperature. *Applied Catalysis A: General*, *592*, p.117413.

50. Song, I., Lee, H., Jeon, S.W., and Kim, D.H., 2020. Controlling catalytic selectivity mediated by stabilization of reactive intermediates in small-pore environments: A study of Mn/TiO_2 in the NH_3-SCR reaction. *ACS Catalysis*, *10*(20), pp.12017-12030.

51. Yang, Y., Hu, Z., Mi, R., Li, D., Yong, X., Yang, H. and Liu, K., 2019. Effect of initial support particle size of MnO_x/TiO_2 catalysts in the selective catalytic reduction of NO with NH_3. *RSC advances*, *9*(9), pp.4682-4692.

52. Xie, S., Li, L., Jin, L., Wu, Y., Liu, H., Qin, Q., Wei, X., Liu, J., Dong, L. and Li, B., 2020. Low temperature high activity of M (M= Ce, Fe, Co, Ni) doped M-Mn/TiO_2 catalysts for NH_3-SCR and in situ DRIFTS for investigating the reaction mechanism. *Applied Surface Science*, *515*, p.146014.

53. Liu, Z., Zhu, J., Li, J., Ma, L. and Woo, S.I., 2014. Novel Mn–Ce–Ti mixed-oxide catalyst for the selective catalytic reduction of NO_x with NH_3. *ACS applied materials & interfaces*, *6*(16), pp.14500-14508.

54. Yang, G., Zhao, H., Luo, X., Shi, K., Zhao, H., Wang, W., Chen, Q., Fan, H. and Wu, T., 2019. Promotion effect and mechanism of the addition of Mo on the enhanced low temperature SCR of NO_x by NH_3 over MnO_x/γ-Al_2O_3 catalysts. *Applied Catalysis B: Environmental*, *245*, pp.743-752.

55. Q. Yang, Y. Ren, L. Zhao, J. Zuo and W. Sun, Appl. Mech. Mater., 2014, 535, 683–687.

56. Jin, R., Liu, Y., Wu, Z., Wang, H. and Gu, T., 2010. Low-temperature selective catalytic reduction of NO with NH_3 over MnCe oxides supported on TiO_2 and Al_2O_3: A comparative study. *Chemosphere*, *78*(9), pp.1160-1166.

57. Pan, X. and Bao, X., 2008. Reactions over catalysts confined in carbon nanotubes. *Chemical communications*, (47), pp.6271-6281.
58. Youn, J.R., Kim, M.J., Lee, S.J., Ryu, I.S., Yoon, H.C., Jeong, S.K., Lee, K. and Jeon, S.G., 2021. The influence of CNTs addition on Mn-Ce/TiO_2 catalyst for low-temperature NH_3-SCR of NO. *Catalysis Communications*, *152*, p.106282.
59. Wang, X., Zheng, Y. and Lin, J., 2013. Highly dispersed Mn–Ce mixed oxides supported on carbon nanotubes for low-temperature NO reduction with NH_3. *Catalysis Communications*, *37*, pp.96-99.
60. Yang, J., Ren, S., Zhang, T., Su, Z., Long, H., Kong, M. and Yao, L., 2020. Iron doped effects on active sites formation over activated carbon supported Mn-Ce oxide catalysts for low-temperature SCR of NO. *Chemical Engineering Journal*, *379*, p.122398.
61. Shen, B., Chen, J., Yue, S. and Li, G., 2015. A comparative study of modified cotton biochar and activated carbon-based catalysts in low temperature SCR. *Fuel*, *156*, pp.47-53.
62. Bueno-López, A., 2014. Diesel soot combustion ceria catalysts. *Applied Catalysis B: Environmental*, *146*, pp.1-11.
63. Li, Q., Yan, X., Shi, M., Wang, Q., Liu, H., Lin, Z. and Huang, X., 2021. Recent advances in metal/ceria catalysts for air pollution control: mechanism insight and application. *Environmental Science: Nano*, *8*(10), pp.2760-2779.
64. Chang, H., Ma, L., Yang, S., Li, J., Chen, L., Wang, W. and Hao, J., 2013. Comparison of preparation methods for ceria catalyst and the effect of surface and bulk sulphates on its activity toward NH_3-SCR. *Journal of hazardous materials*, *262*, pp.782-788.
65. Li, F., Zhang, Y., Xiao, D., Wang, D., Pan, X. and Yang, X., 2010. Hydrothermal Method Prepared Ce-P-O Catalyst for the Selective Catalytic Reduction of NO with NH_3 in a Broad Temperature Range. *ChemCatChem*, *2*(11), pp.1416-1419.

66. Pan, W.G., Zhou, Y., Guo, R.T., Jin, Q., Ding, C.G. and Guo, S.Y., 2013. Effect of cerium precursor on the performance of pure CeO_2 catalysts for selective catalytic reduction of NO with NH_3. *Asian Journal of Chemistry*, *25*(16), p.9079.
67. Tang, C., Zhang, H. and Dong, L., 2016. Ceria-based catalysts for low-temperature selective catalytic reduction of NO with NH_3. *Catalysis science & technology*, *6*(5), pp.1248-1264.
68. Gao, X., Jiang, Y., Zhong, Y., Luo, Z. and Cen, K., 2010. The activity and characterization of CeO_2-TiO_2 catalysts prepared by the sol–gel method for selective catalytic reduction of NO with NH_3. *Journal of Hazardous Materials*, *174*(1-3), pp.734-739.
69. Liu, Z., Zhu, J., Li, J., Ma, L. and Woo, S.I., 2014. Novel Mn–Ce–Ti mixed-oxide catalyst for the selective catalytic reduction of NO_x with NH_3. *ACS applied materials & interfaces*, *6*(16), pp.14500-14508.
70. Chen, L., Si, Z., Wu, X. and Weng, D., 2014. DRIFT study of CuO–CeO_2–TiO_2 mixed oxides for NO_x reduction with NH_3 at low temperatures. *ACS applied materials & interfaces*, *6*(11), pp.8134-8145.
71. Shu, Y., Sun, H., Quan, X. and Chen, S., 2012. Enhancement of catalytic activity over the iron-modified Ce/TiO_2 catalyst for selective catalytic reduction of NO_x with ammonia. *The Journal of Physical Chemistry C*, *116*(48), pp.25319-25327.
72. Fang, C., Zhang, D., Shi, L., Gao, R., Li, H., Ye, L. and Zhang, J., 2013. Highly dispersed CeO_2 on carbon nanotubes for selective catalytic reduction of NO with NH 3. *Catalysis Science & Technology*, *3*(3), pp.803-811.
73. Xu, L., Li, X.S., Crocker, M., Zhang, Z.S., Zhu, A.M. and Shi, C., 2013. A study of the mechanism of low-temperature SCR of NO with NH_3 on MnO_x/CeO_2. *Journal of Molecular Catalysis A: Chemical*, *378*, pp.82-90.

74. Zhu, J., Gao, F., Dong, L., Yu, W., Qi, L., Wang, Z., Dong, L. and Chen, Y., 2010. Studies on surface structure of $M_xO_y/MoO_3/CeO_2$ system (M= Ni, Cu, Fe) and its influence on SCR of NO by NH_3. *Applied Catalysis B: Environmental*, *95*(1-2), pp.144-152.

75. Qi, G. and Yang, R.T., 2003. A superior catalyst for low-temperature NO reduction with NH_3. *Chemical Communications*, (7), pp.848-849.

76. Liu, Z., Yi, Y., Li, J., Woo, S.I., Wang, B., Cao, X. and Li, Z., 2013. A superior catalyst with dual redox cycles for the selective reduction of NO_x by ammonia. *Chemical Communications*, *49*(70), pp.7726-7728.

77. Shan, W., Liu, F., He, H., Shi, X. and Zhang, C., 2011. The Remarkable Improvement of a Ce-Ti based Catalyst for NO_x Abatement, Prepared by a Homogeneous Precipitation Method. *ChemCatChem*, *3*(8), pp.1286-1289.

78. Gao, X., Jiang, Y., Fu, Y., Zhong, Y., Luo, Z. and Cen, K., 2010. Preparation and characterization of CeO_2/TiO_2 catalysts for selective catalytic reduction of NO with NH_3. *Catalysis Communications*, *11*(5), pp.465-469.

79. Liu, C., Chen, L., Chang, H., Ma, L., Peng, Y., Arandiyan, H. and Li, J., 2013. Characterization of CeO_2–WO_3 catalysts prepared by different methods for selective catalytic reduction of NO_x with NH_3. *Catalysis Communications*, *40*, pp.145-148.

80. Xu, W., Yu, Y., Zhang, C. and He, H., 2008. Selective catalytic reduction of NO by NH_3 over a Ce/TiO_2 catalyst. *Catalysis Communications*, *9*(6), pp.1453-1457.

81. Wang, H., Chen, X., Weng, X., Liu, Y., Gao, S. and Wu, Z., 2011. Enhanced catalytic activity for selective catalytic reduction of NO over titanium nanotube-confined CeO_2 catalyst. *Catalysis Communications*, *12*(11), pp.1042-1045.

82. Chen, X., Wang, H., Wu, Z., Liu, Y. and Weng, X., 2011. Novel H2Ti12O25-confined CeO_2 catalyst with remarkable resistance to alkali poisoning based on the "shell protection effect". *The Journal of Physical Chemistry C*, *115*(35), pp.17479-17484.
83. Lu, P., Li, C., Zeng, G., He, L., Peng, D., Cui, H., Li, S. and Zhai, Y., 2010. Low temperature selective catalytic reduction of NO by activated carbon fiber loading lanthanum oxide and ceria. *Applied Catalysis B: Environmental*, *96*(1-2), pp.157-161.
84. Van Kooten, W.E.J., Liang, B., Krijnsen, H.C., Oudshoorn, O.L., Calis, H.P.A. and Van Den Bleek, C.M., 1999. Ce-ZSM-5 catalysts for the selective catalytic reduction of NO_x in stationary diesel exhaust gas. *Applied Catalysis B: Environmental*, *21*(3), pp.203-213.
85. Baerlocher, C., McCusker, L.B. and Olson, D.H., 2007. *Atlas of zeolite framework types*. Elsevier.
86. Gargiulo, N., Caputo, D., Totarella, G., Lisi, L. and Cimino, S., 2018. Me-ZSM-5 monolith foams for the NH_3-SCR of NO. *Catalysis Today*, *304*, pp.112-118.
87. Moliner, M., Franch, C., Palomares, E., Grill, M. and Corma, A., 2012. Cu–SSZ-39, an active and hydrothermally stable catalyst for the selective catalytic reduction of NO_x. *Chemical Communications*, *48*(66), pp.8264-8266.
88. Li, G., Wang, B., Wang, H., Ma, J., Xu, W.Q., Li, Y., Han, Y. and Sun, Q., 2018. Fe and/or Mn oxides supported on fly ash-derived SBA-15 for low-temperature NH_3-SCR. *Catalysis Communications*, *108*, pp.82-87.
89. Wang, Y., Xie, L., Liu, F. and Ruan, W., 2019. Effect of preparation methods on the performance of CuFe-SSZ-13 catalysts for selective catalytic reduction of NO_x with NH_3. *Journal of Environmental Sciences*, *81*, pp.195-204.

90. Hamoud, H.I., Valtchev, V. and Daturi, M., 2019. Selective catalytic reduction of NO_x over Cu-and Fe-exchanged zeolites and their mechanical mixture. *Applied Catalysis B: Environmental*, *250*, pp.419-428.
91. Zhao, S., Huang, L., Jiang, B., Cheng, M., Zhang, J. and Hu, Y., 2018. Stability of Cu–Mn bimetal catalysts based on different zeolites for NO_x removal from diesel engine exhaust. *Chinese Journal of Catalysis*, *39*(4), pp.800-809.
92. Fan, C., Chen, Z., Pang, L., Ming, S., Dong, C., Albert, K.B., Liu, P., Wang, J., Zhu, D., Chen, H. and Li, T., 2018. Steam and alkali resistant Cu-SSZ-13 catalyst for the selective catalytic reduction of NO_x in diesel exhaust. *Chemical Engineering Journal*, *334*, pp.344-354.
93. Shi, X., Guo, J., Shen, T., Fan, A., Liu, Y. and Yuan, S., 2021. Improvement of NH_3-SCR activity and resistance to SO_2 and H_2O by Ce modified La-Mn perovskite catalyst. *Journal of the Taiwan Institute of Chemical Engineers*, *126*, pp.102-111.
94. Fan, A., Jing, Y., Guo, J., Shi, X., Yuan, S. and Li, J., 2022. Investigation of Mn doped perovskite La-Mn oxides for NH_3-SCR activity and SO_2/H_2O resistance. *Fuel*, *310*, p.122237.
95. Fan, X., Hao, L., Gu, X. and Li, S., 2023. Low-Temperature Selective Catalytic Reduction of NO with NH_3 over a Biochar-Supported Perovskite Oxide Catalyst. *Energy & Fuels*, *37*(10), pp.7339-7352.
96. Nie, W., Zhou, W., Li, N., Yuan, M., Yan, J., Hua, Y., Bao, Q., Yu, F. and Niu, W., 2022. The novel monolithic $Pr_{1-x}Ce_xCo_{0.5}Mn_{0.5}O_3$ oxides catalysts for the selective catalytic reduction of NO_x by NH_3. *Catalysis Letters*, *152*(12), pp.3642-3654.
97. Sun, X., Shi, Y., Zhang, W., Li, C., Zhao, Q., Gao, J. and Li, X., 2018. A new type Ni-MOF catalyst with high stability for selective catalytic reduction of NO_x with NH_3. *Catalysis Communications*, *114*, pp.104-108.

98. Wu, X., Liu, J., Liu, X., Wu, X. and Du, Y., 2022. Fabrication of carbon doped Cu-based oxides as superior NH_3-SCR catalysts via employing sodium dodecyl sulfonate intercalating CuMgAl-LDH. *Journal of Catalysis*, *407*, pp.265-280.